Chapter 2

Theoretical Framework

The present chapter provides an overview of the TALYS and EMPIRE statistical model codes, widely utilized for simulating neutron and charged particle-induced reaction cross-sections. The chapter highlights the use of various level density models within these codes for accurate cross-section predictions. Additionally, it briefly introduces optical model potential (OMP) and nuclear level density (NLD) models. These codes were utilized to study neutron-induced reaction cross-sections via neutron activation analysis. TALYS is also highlighted for its role in studying charged particle (proton) induced reactions relevant to astrophysical applications. It also details the use of the spectral distribution method with a shell-model Hamiltonian for calculating NLDs, offering insights into the nuclear reaction mechanisms.

2.1 Overview of Nuclear Reaction Models

Nuclear data holds significant importance in various domains of nuclear physics. The previous chapter highlighted the critical role of nuclear data in nuclear astrophysics and reactor technology applications. A crucial aspect of investigating γ, neutron, light, and heavy-ion induced nuclear reactions is to gain a deeper understanding of the different processes that take place when a high-energy projectile interacts with a target nucleus. The measured data and the resulting physical interpretations facilitate the development of diverse nuclear models that describe various interaction mechanisms. In general, three reaction mechanisms are categorized based on the energy range of the incident particles: compound nucleus (C), pre-equilibrium (P), and direct reaction (D) mechanisms. These mechanisms are incorporated into various reaction models. The different reaction mechanisms are illustrated in Fig. 2.1. Several theoretical models have been developed by researchers for performing nuclear calculations. These models are systematically integrated into modular computational frameworks, referred to as nuclear codes, which are capable of predicting nuclear reaction data with high precision.

Modular codes are frequently employed to compare theoretical predictions with experimental results, helping to validate both the models and the experiments. This is critical for ensuring that simulations are accurate and reliable. By accurately simulating nuclear reactions, modular codes can predict outcomes of experiments and reactions that have not yet been performed, guiding future research and experiments. They help in discovering new nuclear phenomena by providing insights into conditions that are difficult or impossible to achieve experimentally, such as those found in stellar interiors or during supernova explosions.

In this study, we employed the most advanced versions of the TALYS and EMPIRE nuclear model codes. Each code encompasses various nuclear models that can be configured through specific input keywords. The basic details, model descriptions, calculation flow, and an overview of the TALYS and EMPIRE relevant to the current work are outlined in the subsequent sections.

2.2 TALYS: Nuclear Module Overview

TALYS is an advanced computational package widely employed for analyzing and predicting nuclear reaction data. TALYS is designed to simulate various nuclear processes involving γ-rays, neutrons, protons, deuterons, tritons, ^{3}He nuclei, and α-particles up to 200 MeV by taking the reaction parameters from the Reference Input Parameter Library (RIPL database) [2]. The main purpose of TALYS is to connect theoretical models with experimental data, enabling detailed analysis of the interactions between different projectiles and target nuclei. Understanding of fundamental principles is crucial for the development

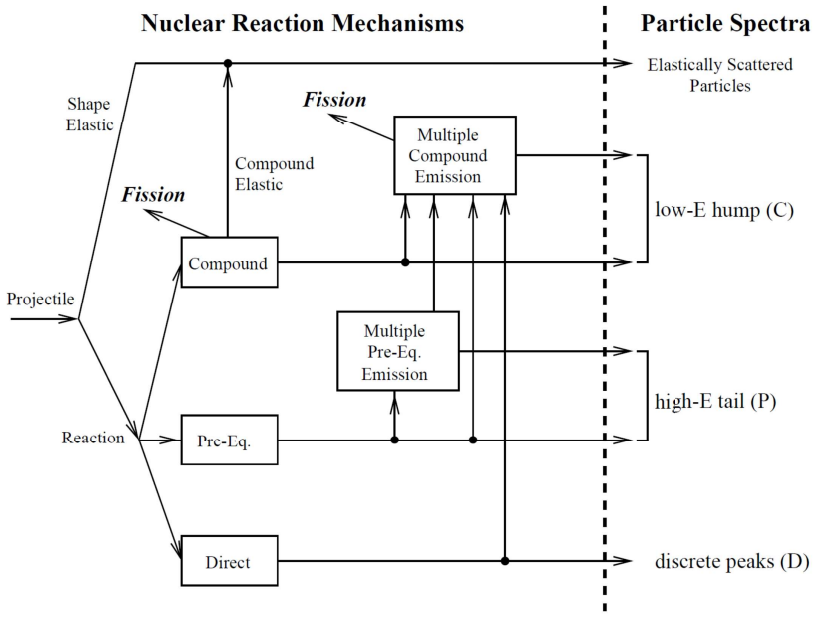

Fig. 2.1: A detailed flow-chart illustrating various nuclear reactions and the corresponding spectra of emitted particles [1].

of nuclear models, which are vital for predicting nuclear reaction data under specific conditions. TALYS can adjust its models to accurately describe available data using adjustable parameters. Key applications that utilize data from the TALYS nuclear reaction simulation code encompass the entire fuel cycle for both existing (GEN-II, III, & III+) and advanced nuclear power reactors (GEN-IV), production of medical isotopes, nuclear fusion research, accelerator-based technologies, various fields of astrophysics, space science, homeland security measures, radiotherapy, analysis of single-event upsets in microprocessors, and geophysical studies [3].

The code accounts for the compound and the non-compound reactions, like pre-equilibrium and the direct reaction mechanism and also the effect of level density parameters as a function of incident particle energy. The OMP parameters are determined using the global potential developed by Koning and Delaroche [4]. The Hauser-Feshbach model is used to account for the compound reaction mechanism [5]. The exciton model developed by Kalbach is used to incorporate pre-equilibrium contribution [6]. For a given projectile + target system, the TALYS code includes all possible outgoing reaction channels. A flow-chart illustrating the TALYS calculation process is presented in Fig. 2.2.

The TALYS-1.95/1.96 package includes six distinct NLD models [7–12], selectable via “ldmodel 1-6" keyword in the input file. These models, identified by the numerical indices 1 to 6 correspond to different theoretical approach for the computation of level densities accounts for:

- 1) constant temperature Fermi gas model (CTFGM) [7] (default);

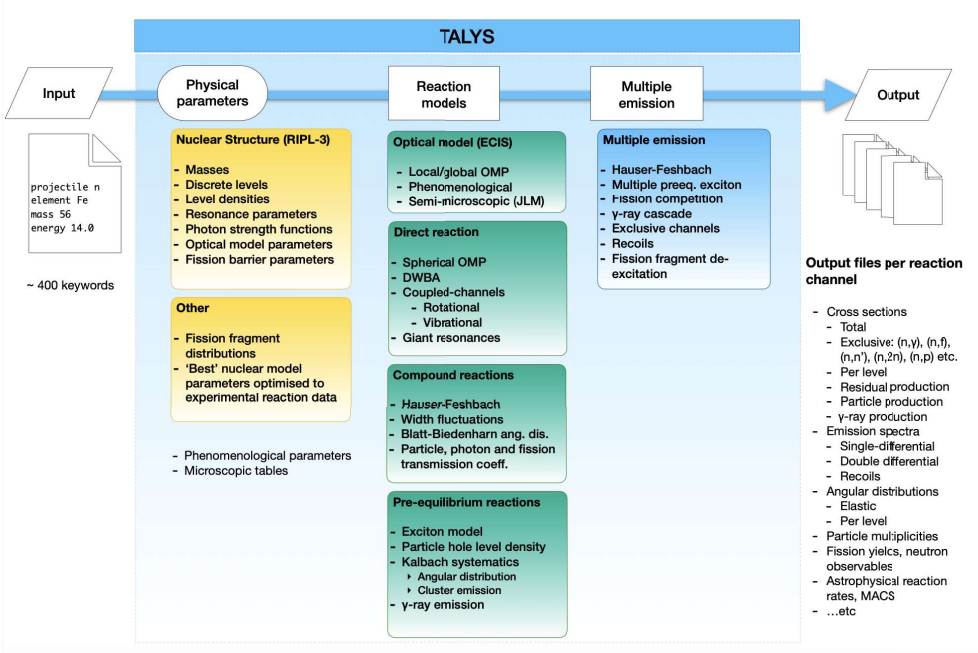

Fig. 2.2: A schematic flow-chart illustrating the calculations performed by the TALYS model [3].

- 2) back-shifted Fermi gas model (BSFGM) [8];
- 3) generalized super-fluid model (GSFM) [9, 10];
- 4)-5) microscopic level densities from Goriely's and Hilaire's tables [11]; and
- 6) microscopic level densities (temperature dependent HFB, Gogny force)[12].

TALYS utilizes adjustable parameters due to the constraints of the models for nuclear reaction mechanisms, making it unfeasible to expect TALYS to ab initio reproduce high-quality experimental data. One significant benefit of the TALYS code is its capacity to produce data for any reaction channel, regardless of prior measurements. The accuracy of the final nuclear reaction simulation is demonstrated by TALYS's ability to interpolate across available experimental data and to extrapolate beyond those data points. We understand that model-predicted nuclear data are not precise. Initially, we focus on quantifying these limitations into measurable numerical uncertainties. By employing the TALYS code, it is now feasible to tackle these uncertainties. This approach has been explored for the astrophysical p-process using the Monte Carlo method, as detailed in Chapter 5.

In summary, the TALYS Nuclear Module stands as a powerful tool for unraveling the complexities of nuclear reactions, contributing significantly to advancements in nuclear physics and astrophysics research. Detailed information about the TALYS code is available in Ref. [3].

TALYS-1.95/1.96 [13] was used to simulate the reaction cross-section of $^{115}\mathrm{In}(\mathrm{n},\mathrm{n}')^{115\mathrm{m}}\mathrm{In}$ and $^{58}\mathrm{Ni}(\mathrm{n},\mathrm{p})^{58}\mathrm{Co}$, while taking into account the effects of level density parameters and several reaction processes, including direct reaction, pre-equilibrium emission, and compound nucleus. These calculations utilized the pre-defined local OMP parameters described by Koning and Delaroche [4]. The Hauser-Feshbach model is used to account for the compound reaction mechanism [5]. The exciton model developed by Kalbach is used to incorporate pre-equilibrium contribution [6]. In our study, LD models were utilized for predicting cross sections, while all other models were set to their default configurations. Each LD model has been utilized and evaluated in order to provide a more accurate representation of the measured results. Fore more detail refer to Chapter 3.

2.3 EMPIRE: Nuclear Module Overview

EMPIRE is another nuclear modular code that incorporates a variety of nuclear models and is specifically developed to execute simulations over a broad spectrum of energies and incident particles. This system is suitable for conducting theoretical analyses of nuclear reactions as well as for the assessment and evaluation of nuclear data. Various projectiles can be utilized, including photons, nucleons, deuterons, tritons, helions ($^3\mathrm{He}$), alpha particles, as well as light and heavy ions. The energy spectrum initiates just above the resonance region for neutron projectiles and spans up to several hundred MeV for reactions induced by heavy ions. The input parameters required for the calculations, including fission barriers, OMP parameters, deformation parameters, discrete level information, nuclear masses, NLDs, and gamma strength functions, were obtained from the RIPL-3 database [2]. The computational results generated by the code were subsequently converted into the ENDF-6 (Evaluated Nuclear Data File) format using the EMPEND utility.

Key reaction models incorporated include the optical model, Coupled Channels and DWBA (ECIS06 and OPTMAN) [14–18], Multi-step Direct (ORION + TRISTAN) [19], and the NVWY Multi-Step Compound model [20]. The Hauser-Feshbach model with the width fluctuation correction is used to incorporate the compound reaction mechanism [6, 21, 22]. The exciton model (PCROSS) [23] or the hybrid Monte Carlo simulation approach [24] using different OMP parameters is used to account for the pre-equilibrium contribution. A flow-chart illustrating the EMPIRE calculation process is presented in Fig. 2.3.

The EMPIRE-3.2.3 package includes four distinct NLD models, selectable via the "LEVDEN 0-3" keyword in the input file. These models, identified by the numerical indices 0 to 3 correspond to different theoretical approach for the computation of level densities accounts for:

- 0) Enhanced generalised superfluid model [26] (default);

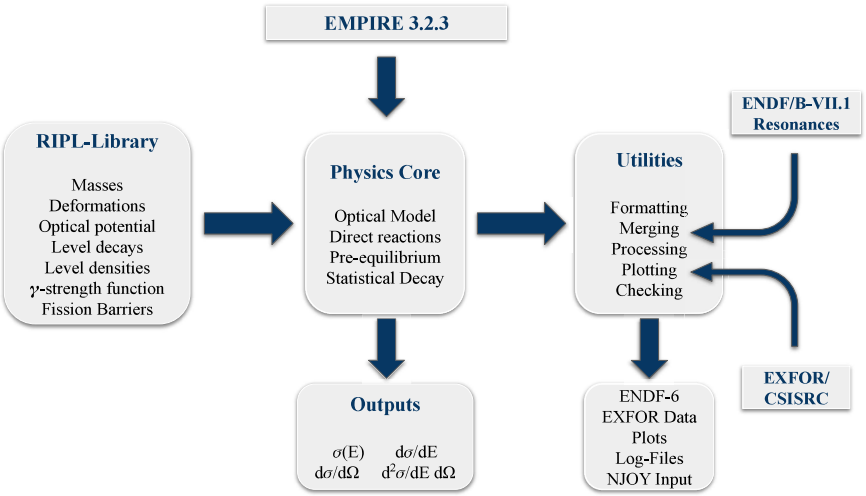

Fig. 2.3: A schematic flow-chart illustrating the calculations performed by the EMPIRE model [25].

- 1) Generalised superfluid model [9, 10];
- 2) Gilbert-Cameron level densities [27];
- 3) RIPL-3 microscopic HFB level densities.

Further detailed information about the code is provided in the EMPIRE manual [28].

EMPIRE-3.2.3 [25] was used to simulate the reaction cross-section of $^{115}\mathrm{In}(\mathrm{n},\mathrm{n}')^{115\mathrm{m}}\mathrm{In}$, while taking into account the effects of level density parameters and several reaction processes, including direct reaction, pre-equilibrium emission, and compound nucleus. In our study, LD models were utilized for predicting cross sections, while all other models were set to their default configurations. Each LD model has been utilized and evaluated in order to provide a more accurate representation of the measured results. Fore more detail refer to Chapter 3.

2.4 Shell Model Calculations

Calculations of NLDs can be performed using the spectral distribution method (SDM) [29–34] with a shell-model Hamiltonian that includes a realistic residual interaction. SDM is widely used in nuclear physics to gain insights into the structure and behaviour of atomic nuclei in various fields, such as nuclear astrophysics, nuclear energy, and nuclear medicine. This involves determining the energy levels of the nucleus, analyzing the resulting energy spectrum, and applying statistical methods to obtain a smooth function that describes the NLDs as a function of energy. The NLD essentially quantifies the overall number of nuclear states within a particular nucleus for a defined excitation energy. A variety

of approaches exist for determining NLDs, ranging from basic phenomenological models that utilize a noninteracting degenerate Fermi gas framework [7, 8] to more advanced mean-field theoretical descriptions [11]. However, in the shell model, the configuration mixing through the residual interaction naturally accounts for the collective excitations.

Within the SDM, one begins by calculating the first and second moments of the Hamiltonian across the entire configuration space. These moments are then employed to construct a Gaussian distribution of the energy levels, which is subsequently used to determine the level density. For a specific isotope characterized by proton number Z and neutron number N, the valence nucleons can be arranged in numerous ways across the available orbitals. Each distinct arrangement is referred to as a partition p, which encompasses $D_{\alpha p}$ many-body states with specific quantum numbers α. The energy distribution of states within a partition is influenced by the interactions within that partition. The statistical average of an operator $\hat{O}$ over these states is defined via the corresponding trace for each partition,

$$\langle \hat{O} \rangle = \frac{\mathrm{Tr}^{\alpha p}(\hat{O})}{D_{\alpha p}}. \tag{2.1}$$

The centroid energy of a partition represents the first moment of the Hamiltonian,

$$E_{\alpha p} = \langle \hat{H} \rangle_p = \frac{\mathrm{Tr}^{\alpha p}(\hat{H})}{D_{\alpha p}}. \tag{2.2}$$

This is derived directly from the diagonal elements of the Hamiltonian matrix. The second moment of the Hamiltonian,

$$\sigma^2_{\alpha p} = \langle H^2 \rangle_{\alpha p} - E^2_{\alpha p} = \frac{\mathrm{Tr}^{\alpha p}\, H^2}{D_{\alpha p}} - E^2_{\alpha p}, \tag{2.3}$$

is determined by the off-diagonal components of the Hamiltonian matrix, which include interactions between partitions. Diagonalizing the matrix is not needed, as this quantity can be directly obtained from the Hamiltonian matrix. The resulting distributions closely approximate Gaussian profiles, illustrating the intricate manifestations of quantum complexity and chaotization [35–38]. Ultimately, the level density $\rho(E;\alpha)$ is determined by summing Gaussian contributions weighted by their respective dimensions across all partitions at a given energy E and with specific quantum numbers α,

$$\rho(E;\alpha) = \sum_p D_{\alpha p}\, G_{\alpha p}(E). \tag{2.4}$$

For optimal results, finite-range or truncated Gaussians are employed for each partition:

$$G_{\alpha p}(E) = G(E - E_{\alpha p} + E_{g.s.}; \sigma_{\alpha p}). \tag{2.5}$$

These Gaussians are truncated at a distance of approximately $2.6\,\sigma_{\alpha\mathrm{p}}$ from their centroids to remove unphysical tails, followed by renormalization [39].

In the present work, the realistic NLDs for the $^{58}\mathrm{Ni}$ and other nuclei involved in the reaction and population of the radionuclides in different channels were obtained by employing the SDM followed by an appropriate parity equilibration scheme for the pf-model space [40, 41] to calculate the $^{58}\mathrm{Ni}(\mathrm{n},\mathrm{p})^{58}\mathrm{Co}$ reaction cross-sections. For more detail refer to to Section 3.5.3.

✠ ✠ ✠ ✠

References

[1] A. Koning, S. Hilaire, and M. Duijvestijn, NRG-1755 ZG Petten, The Netherlands (2019).

[2] R. Capote, M. Herman, P. Obložinskỳ, et al., Nuclear Data Sheets **110**(12), 3107–3214 (2009).

[3] A. Koning, S. Hilaire, and S. Goriely, The European Physical Journal A **59**(6), 131 (2023).

[4] A. Koning and J. Delaroche, Nuclear Physics A **713**(3-4), 231–310 (2003).

[5] W. Hauser and H. Feshbach, Physical review **87**(2), 366 (1952).

[6] C. Kalbach, Physical Review C **33**(3), 818 (1986).

[7] A. Gilbert and A. Cameron, Canadian Journal of Physics **43**(8), 1446–1496 (1965).

[8] W. Dilg, W. Schantl, H. Vonach, et al., Nuclear Physics A **217**(2), 269–298 (1973).

[9] A. Ignatyuk, K. Istekov, and G. Smirenkin, Sov. J. Nucl. Phys.(Engl. Transl.);(United States) **30**(5) (1979).

[10] A. Ignatyuk, J. Weil, S. Raman, et al., Physical Review C **47**(4), 1504 (1993).

[11] S. Goriely, S. Hilaire, and A. Koning, Physical Review C **78**(6), 064307 (2008).

[12] S. Hilaire, M. Girod, S. Goriely, et al., Physical Review C **86**(6), 064317 (2012).

[13] A. Koning, S. Hilaire, and M. C. Duijvestijn, in International Conference on Nuclear Data for Science and Technology (EDP Sciences, 2007), pp. 211–214.

[14] J. Raynal, Technical Report IAEA-SMR-9/8, Presented at the International Seminar Course on Computing as a Language of Physics, Trieste, Italy, 2 Aug 1971 (IAEA, Vienna), pp. 281–322.

[15] J. Raynal, International Centre for Theoretical Physics, Trieste (Italy), Vienna, 1972.

[16] E. S. Soukhovitskii, G. B. Morogovskii, S. Chiba, et al., (2004).

[17] E. S. Soukhovitskiı, S. Chiba, O. Iwamoto, et al., tech. rep. (Technical report JAERI-Data/Code 2005-002, Japan Atomic Energy Research . . ., 2005).

[18] E. S. Soukhovitskiı, S. Chiba, R. Capote, et al., Manual Version **10**, 2008–025 (2008).

[19] H. Lenske and H. H. Wolter, Private communication, n.d.

[20] H. Nishioka, J. Verbaarschot, H. Weidenmüller, et al., Annals of Physics **172**(1), 67–99 (1986).

[21] H. Hofmann, J. Richert, J. Tepel, et al., Annals of Physics **90**(2), 403–437 (1975).

[22] A. Adam and L. Jeki, Acta Physica Academiae Scientiarum Hungaricae **26**(4), 335–338 (1969).

[23] J. J. Griffin, Physical Review Letters **17**, 478 (1966).

[24] M. B. Chadwick, Private communication to M. Herman, 2000.

[25] M. Herman, R. Capote, B. Carlson, et al., Nuclear data sheets **108**(12), 2655–2715 (2007).

[26] A. D'Arrigo, G. Giardina, M. Herman, et al., Journal of Physics G: Nuclear and Particle Physics **20**(2), 365 (1994).

[27] A. Iljinov, M. Mebel, N. Bianchi, et al., Nuclear Physics A **543**(3), 517–557 (1992).

[28] M. Herman, R. Capote, and M. Sin, tech. rep. (International Atomic Energy Agency, 2013).

[29] F. S. Chang, J. B. French, and T. H. Thio, Annals of Physics **66**(1), 137–188 (1971).

[30] J. French and K. Ratcliff, Physical Review C **3**(1), 94 (1971).

[31] V. Kota and K. Kar, Pramana **32**, 647–692 (1989).

[32] V. Kota and D. Majumdar, Nuclear Physics A **604**(2), 129–162 (1996).

[33] M. Horoi, J. Kaiser, and V. Zelevinsky, Physical Review C **67**(5), 054309 (2003).

[34] M. Horoi, M. Ghita, and V. Zelevinsky, Physical Review C **69**(4), 041307 (2004).

[35] V. Kota (World Scientific, 2010).

[36] S. S. M. Wong (Oxford University Press Inc, 1986).

[37] T. A. Brody, J. Flores, J. B. French, et al., Reviews of Modern Physics **53**(3), 385 (1981).

[38] K. Mon and J. B. French, Annals of Physics **95**(1), 90–111 (1975).

[39] R. A. Sen'kov, M. Horoi, and V. G. Zelevinsky, Computer Physics Communications **184**(1), 215–221 (2013).

[40] Sangeeta, T. Ghosh, B. Maheshwari, et al., Physical Review C **105**, 044320 (2022).

[41] W. Ormand and B. Brown, Physical Review C **102**(1), 014315 (2020).